AIP Advances

Magnetic-field and temperature dependence of anomalous Hall effect in Pt/Cr_2O_3/Pt trilayer

Cite as: AIP Advances **12**, 035216 (2022); https://doi.org/10.1063/9.0000253
Submitted: 25 October 2021 • Accepted: 19 November 2021 • Published Online: 09 March 2022

Xinrui Wang, Kentaro Toyoki, Ryoichi Nakatani, et al.

Magnetic-field and temperature dependence of anomalous Hall effect in Pt/Cr_2O_3/Pt trilayer

Cite as: AIP Advances 12, 035216 (2022); doi: 10.1063/9.0000253
Presented: 27 December 2021 • Submitted: 25 October 2021 •
Accepted: 19 November 2021 • Published Online: 9 March 2022

Xinrui Wang,[1] Kentaro Toyoki,[1] Ryoichi Nakatani,[1,2] and Yu Shiratsuchi[1,2,a)]

AFFILIATIONS

[1] Department of Materials Science and Engineering, Graduate School of Engineering, Osaka University, 2-1 Yamadaoka, Suita, Osaka 565-0871, Japan
[2] Center for Spintronics Research Network, Graduate School of Engineering Science, Osaka University, Toyonaka, Osaka 560-8531, Japan

Note: This paper was presented at the 15th Joint MMM-Intermag Conference.
[a)] **Author to whom correspondence should be addressed:** shiratsuchi@mat.eng.osaka-u.ac.jp

ABSTRACT

The Pt/Cr_2O_3 interface exhibits a variety of spin-related phenomena. In this study, we investigated the anomalous Hall effect (AHE) of a Pt/40-nm-thick Cr_2O_3/Pt trilayer grown on Al_2O_3(0001), where Cr_2O_3 is an antiferromagnetic (AFM) insulator. All layers were grown epitaxially on the substrate, and X-ray reflectivity measurement showed an interfacial roughness of approximately 0.2 nm at each interface. The AHE resistance showed a nonlinear magnetic-field dependence at 300 K. Below 250 K, a clear hysteresis with coercivity was observed. The coercivity was approximately 7 T above 150 K and approximately 6 T below 100 K. The remanent AHE resistance shows a finite value below 285 K. The temperature dependence forms a broad peak with a maximum at approximately 200 K and gradually decreases with decreasing temperature. This temperature dependence is similar to that reported for the interfacial magnetic moment on Cr_2O_3(0001). Based on these results, the remanent AHE coupled with the AFM order parameter or the Néel vector was successfully detected in the 40-nm-thick Cr_2O_3 layer grown on the conductive layer.

I. INTRODUCTION

Antiferromagnetic (AFM) spintronics has been an area of active research.[1] The absence of net magnetization makes antiferromagnets robust against perturbations by an external magnetic field. In addition, the ultrafast resonant frequency of AFM resonance can be exploited to achieve THz emission devices. Because of the absence of net magnetization, controlling and detecting AFM moments or the Néel vector are difficult challenges. To date, some advanced techniques such as the spin–orbit torque,[2] magnetoelectric (ME) effect,[3,4] and piezo-electric strain[5] have been used to control AFM moments. For the detection of AFM moment/domains, previous studies have used spin-related transport phenomena such as the anomalous Hall effect (AHE)[3,6] and planar Hall effect,[2] optical techniques,[7–9] and synchrotron measurements based on magnetic linear/circular dichroism.[10–12]

The heavy metal (HM)/Cr_2O_3 interface, where Cr_2O_3 is an AFM insulator, exhibits a variety of spin-related transport phenomena, such as non-linear AHE[6,13] and the topological Hall effect.[14] Cr_2O_3 is a particularly important material for AFM spintronics because of the ME coupling between antiferromagnetism and ferroelectricity,[15,16] and the ME-induced switching of the AFM order parameter has been widely studied.[16] The detection of the AFM order parameter of Cr_2O_3 based on transport measurements was first proposed by Kosub *et al.*[6] using the Pt/Cr_2O_3 bilayer, where the remanent AHE resistance was assumed to be an imprint of the AFM order parameter. This technique has been extended to the detection of the ME-controlled AFM order parameter.[4] Although Kosub *et al.*[6] assumed that the induced Pt moment exchange-coupled with the surface magnetization was responsible for the remanent AHE resistance, other mechanisms such as the interfacial chiral spin structure[13] have been proposed. The detailed physical mechanism of AHE manifestation is still controversial.

The Cr_2O_3 thickness is an important parameter, and a reduction in thickness is desirable for manufacturing. The previously studied HM/Cr_2O_3 bilayer typically has a Cr_2O_3 layer of thickness

20–50 nm.[14,17,18] However, this structure was directly grown on a single-crystalline α-Al_2O_3 substrate, without a conductive underlayer, which is essential for applying voltage. In contrast, the ME Cr_2O_3 films grown on a conductive underlayer typically employed a Cr_2O_3 layer of 200–250 nm thickness.[3,5] The difficulty in reducing the Cr_2O_3 thickness on the conductive underlayer is partly due to the persistence of the good insulating property in the low-thickness regime. In the present study, we fabricated a Pt/40-nm-thick Cr_2O_3/Pt trilayer with high resistance. Using this trilayer, we investigated the AHE as a function of the magnetic field and temperature. In addition to the reduction of Cr_2O_3 thickness, our investigations cover a high magnetic field above 6 T and a wide temperature range of 10–310 K, in contrast to previous reports where the applied magnetic field strength is typically below 3 T[18] and the temperature regime is typically above 250 K.[3,5,18]

II. EXPERIMENTAL

The Pt/Cr_2O_3/Pt trilayer was grown on an α-Al_2O_3(0001) substrate using the DC magnetron sputtering method. The base pressure of the deposition chamber was below 1×10^{-6} Pa. A 20-nm-thick Pt buffer layer was deposited on the substrate at 873 K. On the Pt buffer layer, a 40-nm-thick Cr_2O_3 layer was deposited by reactive sputtering using a gas mixture of Ar and O_2. The deposition temperature of Cr_2O_3 was 773 K. Subsequently, a 2-nm-thick Pt layer was deposited at room temperature. The surface structure of each layer was examined by reflection high-energy electron diffraction (RHEED). The RHEED observation was performed in a different chamber connected to the deposition chamber via the gate valve so that the film could be transferred without exposure to air. X-ray reflectivity (XRR) and high-angle X-ray diffraction (XRD) measurements were performed to determine the interface roughness and crystalline orientation. These measurements were performed using Cu K_α irradiation.

For the AHE measurements, the film was patterned into a micro-Hall device with a length of 40 μm and a width of 2 μm. Microfabrication was performed using photolithography and Ar ion milling. The fabricated device was equipped with a bottom electrode to measure the electrical resistance of the Cr_2O_3 layer. In our device, a 20-nm-thick Pt buffer layer was used as the bottom electrode. The leakage current at room temperature was 23 nA at 0.5 V (12.5 MV/m). That is the resistivity was 2×10^5 Ωm. We measured the AHE resistance R_{AHE} as a function of magnetic field and temperature. To eliminate the artificial offset caused by imperfections in the device structure, we employed a spinning-current AHE measurement using a multiplexer, as proposed by Kosub *et al.*[6] The details of the measurement technique were reported by Kosub *et al.*[6] The error bar of R_{AHE} was calculated using the standard deviation of the Hall voltage measured with four configurations in the spinning-current AHE measurement. In the previous study by Kosub *et al.*,[6] the applied magnetic field strength was insufficient to achieve the switching of the interfacial AFM moment, and minor loops were measured. In this study, we applied a high magnetic field up to $\mu_0 H$ = 9 T in an attempt to reverse the interfacial AFM moment. The temperature dependence of the remanent AHE resistance was also measured. In these measurements, the sample was heated to 310 K, which is above the Néel temperature (T_N) of bulk Cr_2O_3 (307 K[19]). At 310 K, a magnetic field of $\mu_0 H_{cool}$ ranging from −2 to +2 T was applied. In maintaining $\mu_0 H$, the sample was cooled to 10 or 270 K. After reaching the target temperature, the magnetic field was removed. Subsequently, the remanent R_{AHE}, R_{AHE_Rem}, was measured with increasing temperature. The sense current used to measure R_{AHE} was set to 1 mA. The direction of the applied field was perpendicular to the film plane. The positive direction of H was defined as the direction from the bottom electrode to the top electrode.

III. RESULTS AND DISCUSSION

First, we present the results of the structural analysis based on the RHEED observations as well as XRR and XRD profiles. Figures 1(a) and 1(b) show the RHEED images of the Cr_2O_3 layer for the [11$\bar{2}$0] azimuth and the [1$\bar{1}$00] azimuth, respectively. Streak patterns were observed for both the azimuths. The spacings between streaks were different for the orthogonal electron azimuth. The RHEED patterns indicate the epitaxial growth of the Cr_2O_3(0001) layer and a flat surface. The XRR profile (not shown) shows a clear oscillation above $2\theta = 10^\circ$, and theoretical fitting provides the interface roughness of each layer as approximately 0.2 nm. In the $2\theta/\omega$ XRD profile (not shown), no diffraction peaks other than those of Pt(111), Cr_2O_3(0006), and the substrate were observed. The Laue fringes were superimposed around the main diffraction peak, indicating good crystalline quality.

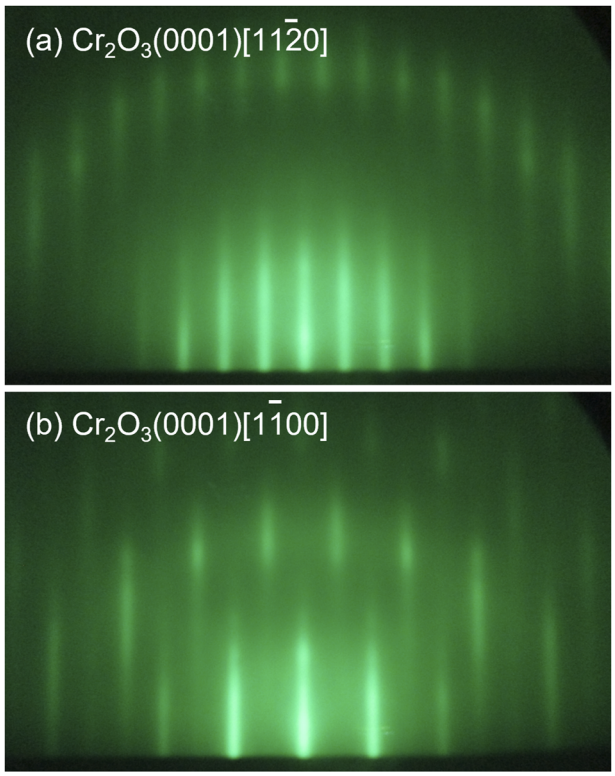

FIG. 1. (a) $[11\bar{2}0]_{substrate}$-azimuthal and (b) $[1\bar{1}00]_{substrate}$-azimuthal RHEED images of the Cr_2O_3 surface.

Figure 2 shows a series of AHE loops, that is R_{AHE}–$\mu_0 H$ curves measured at various temperatures. At 300 K (Fig. 2(a)), R_{AHE} exhibits non-linear behavior with respect to $\mu_0 H$. In the $\mu_0 H$ range from −0.2 T to 0.2 T, R_{AHE} shows a sharp increase, and above 0.5 T, R_{AHE} starts to decrease. R_{AHE} decreases linearly above 0.5 T, presumably due to the ordinal Hall effect from Pt. A similar AHE loop was previously observed in Pt/Cr_2O_3[13] and Ta/Cr_2O_3[17] bilayers directly deposited on an α-Al_2O_3 substrate. This type of AHE loop was observed above T_N.[13,17] The physical mechanism of the non-linear AHE above T_N is still controversial, as mentioned above. Notably, R_{AHE_R} is zero within the error at 300 K, which is also in agreement with a previous report for a Pt/200-nm-thick Cr_2O_3 bilayer.[6] The sign of R_{AHE} is the same as that reported by Moriyama *et al.*,[13] Cheng *et al.*,[14] and Ji *et al.*[17] but is opposite to that in Ref. 6. This is probably because of the definition of the Hall voltage.

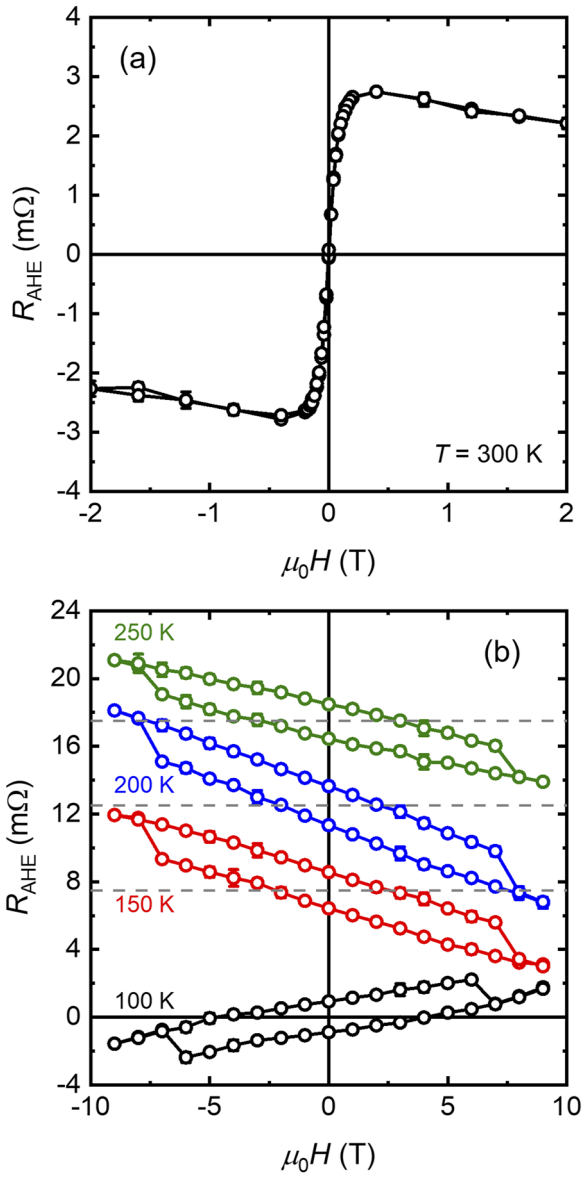

FIG. 2. (a) AHE loop measured at 300 K. (b) Series of AHE loops measured at 100 K (black), 150 K (red), 200 K (blue), and 250 K (green), respectively. The loops are shifted in the vertical direction for easy visibility. The gray horizontal dotted lines represent the center position of each loop.

With decreasing temperature, the AHE loops show clear hysteresis with sizable coercivity (Fig. 2(b)). The sign of R_{AHE_Rem} is negative, opposite to that reported by Kosub *et al.*,[6] as mentioned above. The coercivity is approximately 7 T above 150 K and approximately 6 T below 100 K. Although the coercivity must be precisely determined, it is likely that the coercivity is insensitive to temperature. It should be mentioned that the spin-flop transition may occur in a similar field regime in bulk Cr_2O_3.[20] The relationship between coercivity and the spin-flop field is currently unclear. The thickness and angular dependence of coercivity might provide deeper insight, and this is a subject for future research. It can also be seen that the linear contribution changes sign with decreasing temperature. This tendency is maintained up to 10 K (not shown), and the slope reaches approximately +2.8 mΩ/T at 10 K. At present, the reason for the temperature dependence of the linear contribution is unclear.

To eliminate the linear contribution to R_{AHE}, we measured the temperature dependence of R_{AHE_Rem} under various $\mu_0 H_{cool}$ conditions. Figure 3(a) shows the temperature dependence of R_{AHE_Rem} with $\mu_0 H_{cool}$ = ±2 T. It is first observed that R_{AHE_Rem} is reversed by reversing $\mu_0 H_{cool}$. $|R_{AHE\_Rem}|$ is approximately 0.5 mΩ at 10 K, increases with increasing temperature up to 200 K, and forms a broad peak. Above approximately 225 K, $|R_{AHE\_Rem}|$ starts to decrease and becomes zero at 285 K, that is T_N is 285 K. T_N is similar to the previously reported value of ~280 K for the Pt/20-nm-thick Cr_2O_3 bilayer based on spin Hall magnetoresistance (SMR) measurements.[21] The temperature dependence of R_{AHE_Rem} is reminiscent of that of the exchange bias in a ferromagnetic layer/Cr_2O_3(0001) thin film[22,23] and that of the axial magnetic moment of a Pt/200-nm-thick Cr_2O_3 bilayer,[23] except for the T_N value. The critical exponent β was also estimated in the temperature regime of T/T_N = 0.95–1.00, and β = 0.338 ± 0.033 was obtained.[23] The β value was also similar to that in a previous report.[6] It should be noted that, in general, the anomalous Hall coefficient depends on the longitudinal resistivity σ_{xx} and is not constant with temperature change. However, if the thin film is in the "good-metal regime," i.e., $\sigma_{xx} \sim 10^4$–10^6 $(\Omega\text{cm})^{-1}$,[24] and the probed temperature range is sufficiently small, the anomalous Hall conductivity, ρ_{xy}/ρ_{xx}^2 (where ρ_{xy} and ρ_{xx} are the Hall resistivity and longitudinal resistivity, respectively), is independent of the longitudinal resistance. The σ_{xx} of the device used was approximately 1×10^5 $(\Omega\text{cm})^{-1}$ and did not show any anomaly around T_N. Therefore, the critical exponent can be determined using AHE measurements.[25]

We further investigated the $\mu_0 H_{cool}$ dependence of R_{AHE_Rem}. Figure 3(b) shows the change in R_{AHE_Rem} at 270 K with $\mu_0 H_{cool}$. R_{AHE_Rem} shows a sigmoid-like $\mu_0 H_{cool}$ dependence, similar to a previous report.[6] As shown in the inset of Fig. 3(b), the AHE loops at 270 K do not show hysteresis below 6 T, and R_{AHE_Rem} persists after applying a magnetic field of ±6 T. Therefore, the sigmoid-like behavior suggests that two AFM domain states are selected upon forming the AFM order.

It should be noted that to enable the effects reported here, a single-domain state of the Cr_2O_3 layer is required by symmetry to

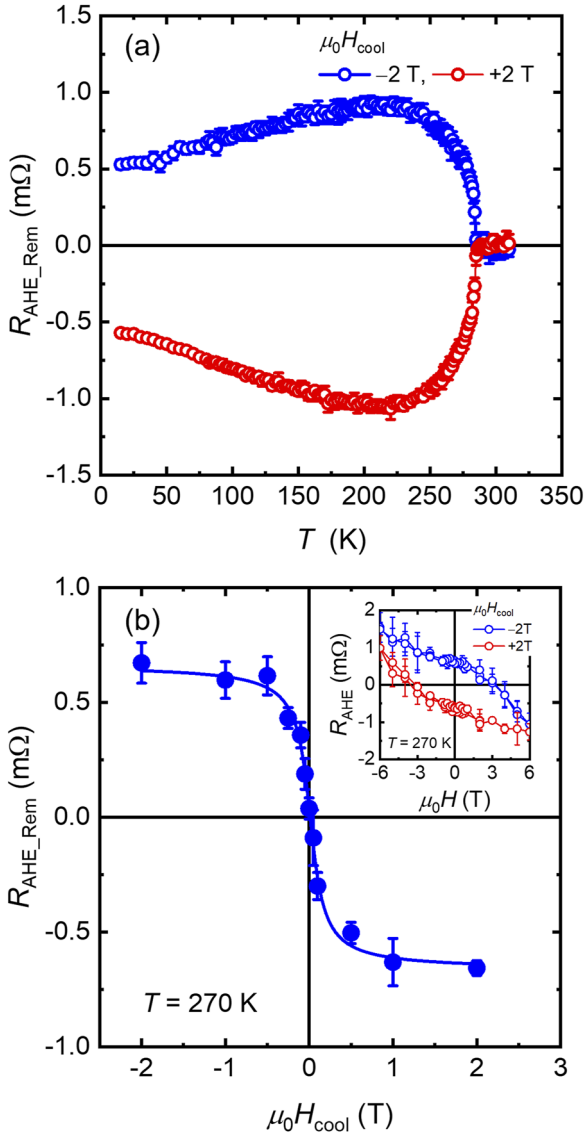

FIG. 3. (a) Temperature dependence of R_{AHE_Rem} for $\mu_0 H_{cool}$ values of +2 T (red) and −2 T (blue). (b) $\mu_0 H_{cool}$ dependence of R_{AHE_Rem} at 270 K. The inset shows the AHE loops measured at 270 K for $\mu_0 H_{cool}$ values of +2 T (red) and −2 T (blue).

have surface magnetization (boundary magnetization).[4,26–28] At the same time, we are aware of the importance of confirming the absence of net magnetization and that the observed AHE is responsible for neither impurity- nor defect-induced magnetization. Because of this instrumental limitation, we could not measure the magnetization curves with the highest $\mu_0 H$ above 6 T. Nonetheless, we previously showed that the nonlinear AHE loop does not rely on either the spin polarization of Pt or the magnetic susceptibility of the interfacial Cr moment in the Pt/Cr_2O_3 bilayer fabricated using the same method with an identical deposition system.[13] A similar feature for the film studied in this paper will be investigated, for example, by X-ray magnetic circular dichroism in the near future.

IV. SUMMARY

The AHE of the Pt/40-nm-thick Cr_2O_3/Pt trilayer was investigated. The 40-nm-thick Cr_2O_3 layer grown on the Pt(111) buffer layer showed a high electrical resistivity of approximately 1×10^6 Ωcm. XRR and XRD profiles revealed an interface roughness of approximately 0.2 nm and good crystalline quality, which was sufficient to produce Laue fringes. We found that the AHE loop showed non-linear behavior at 300 K, similar to a previous report using Pt/Cr_2O_3 bilayers. We also observed clear hysteresis with a coercivity of approximately 6–7 T below 250 K. The temperature dependence of R_{AHE_Rem} resembles that of the exchange bias field in the FM/Cr_2O_3 system and that of the axial magnetic moment in the Cr_2O_3(0001) film. The T_N at which R_{AHE_Rem} becomes zero was 285 K, which is similar to the T_N of the Pt/20-nm-thick Cr_2O_3 bilayer. The temperature dependence of R_{AHE_Rem} with various $\mu_0 H_{cool}$ values suggests the selectivity of the AFM domain state. The results indicate that R_{AHE_Rem} is an imprint of the AFM order parameter, that is the Néel vector.

ACKNOWLEDGMENTS

This work was partly supported by JSPS KAKENHI (Project No. 19H00825).

AUTHOR DECLARATIONS

Conflict of Interest

The authors have no conflicts to disclose.

DATA AVAILABILITY

The data that support the findings of this study are available from the corresponding author upon reasonable request.

REFERENCES

[1] V. Baltz, A. Manchon, M. Tsoi, T. Moriyama, T. Ono, and Y. Tserkovnyak, Rev. Mod. Phys. **90**, 015005 (2018).
[2] P. Wadley, B. Howells, J. Železný, C. Andrews, V. Hills, R. P. Campion, V. Novák, K. Olejník, F. Maccherozzi, S. S. Dhesi, S. Y. Martin, T. Wagner, J. Wunderlich, F. Freimuth, Y. Mokrousov, J. Kuneš, J. S. Chauhan, M. J. Grzybowski, A. W. Rushforth, K. W. Edmonds, B. L. Gallagher, and T. Jungwirth, Science **351**, 587 (2016).
[3] T. Kosub, M. Kopte, R. Hühne, P. Appel, B. Shields, P. Maletinsky, R. Hübner, M. O. Liedke, J. Fassbender, O. G. Schmidt, and D. Makarov, Nature Commun. **8**, 13985 (2017).
[4] X. He, Y. Wang, N. Wu, A. N. Caruso, E. Vescovo, K. D. Belashchenko, P. A. Dowben, and C. Binek, Nature Mater. **9**, 579 (2010).
[5] A. Mahmood, W. Echtenkamp, M. Street, J.-L. Wang, S. Cao, T. Komesu, P. A. Dowben, P. Buragohain, H. Lu, A. Gruverman, A. Parthasarathy, S. Rakheja, and C. Binek, Nature Commun. **12**, 1674 (2021).
[6] T. Kosub, M. Kopte, F. Radu, O. G. Schmidt, and D. Makarov, Phys. Rev. Lett. **115**, 097201 (2015).
[7] H. Kondoh and T. Takeda, J. Phys. Soc. Jpn. **19**, 2041 (1964).
[8] M. Fiebig, D. Fröhlich, G. Sluyterman v. L., and R. V. Pisarev, Appl. Phys. Lett. **66**, 2906 (1995).
[9] J. Xu, C. Zhou, M. Jia, D. Shi, C. Liu, H. Chen, G. Chen, G. Zhang, Y. Liang, J. Li, W. Zhang, and Y. Wu, Phys. Rev. B **100**, 134413 (2019).
[10] K. Arai, T. Okuda, A. Tanaka, M. Kotsugi, K. Fukumoto, T. Ohkochi, T. Nakamura, T. Matsushita, T. Muro, M. Oura, Y. Senba, H. Ohashi, A. Kakizaki, C. Mitsumata, and T. Kinoshita, Phys. Rev. B **85**, 104418 (2012).

[11]N. Wu, X. He, A. L. Wysocki, U. Lanke, T. Komesu, K. D. Belashchenko, C. Binek, and P. A. Dowben, Phys. Rev. Lett. **106**, 087202 (2011).
[12]Y. Shiratsuchi, Y. Kotani, S. Yoshida, Y. Yoshikawa, K. Toyoki, A. Kobane, R. Nakatani, and T. Nakamura, AIMS Mater. Sci. **2**, 484 (2015).
[13]T. Moriyama, Y. Shiratsuchi, T. Iino, H. Aono, M. Suzuki, T. Nakamura, Y. Kotani, R. Nakatani, K. Nakamura, and T. Ono, Phys. Rev. Applied **13**, 034052 (2020).
[14]Y. Cheng, S. Yu, M. Zhu, J. Hwang, and F. Yang, Phys. Rev. Lett. **123**, 237206 (2019).
[15]M. Fiebig, J. Phys. D: Appl. Phys. **38**, R123 (2005).
[16]Y. Shriatsuchi, K. Toyoki, and R. Nakatani, J. Phys. Condens. Matter. **33**, 243001 (2021).
[17]Y. Ji, J. Miao, Y. M. Zhu, K. K. Meng, X. G. Xu, J. K. Chen, Y. Wu, and Y. Jiang, Appl. Phys. Lett. **112**, 232404 (2018).
[18]J. Wang, W. Echtenkamp, A. Mahmood, and C. Binek, J. Magn. Magn. Mater. **486**, 165262 (2019).
[19]S. Foner, Phys. Rev. **130**, 183 (1963).
[20]S. Foner and M. Hanabusa, J. Appl. Phys. **34**, 1246 (1963).
[21]T. Iino, T. Moriyama, H. Iwaki, H. Aono, Y. Shiratsuchi, and T. Ono, Appl. Phys. Lett. **114**, 022402 (2019).
[22]Y. Shiratsuchi and R. Nakatani, Mater. Trans. **57**, 781 (2016).
[23]Supplementary information of Ref. 4.
[24]N. Nagaosa, J. Sinova, S. Onoda, A. H. MacDonald, and N. P. Ong, Rev. Mod. Phys. **82**, 1539 (2010).
[25]D. Chiba, S. Fukami, K. Shimamura, N. Ishiwata, K. Kobayashi, and T. Ono, Nature Mater. **10**, 853 (2011).
[26]A. F. Andreev, JETP Lett. **63**, 758 (1996).
[27]K. D. Belashchenko, Phys. Rev. Lett. **105**, 147204 (2010).
[28]K. Toyoki, Y. Shiratsuchi, T. Nakamura, C. Mitsumata, S. Harimoto, Y. Takechi, T. Nishimura, H. Nomura, and R. Nakatani, Appl. Phys. Express **7**, 114201 (2014).